Separation Science and Technology
Publication details, including instructions for authors and subscription information:
http://www.informaworld.com/smpp/title~content=t713708471

Simulation and Optimization for Power Plant Flue Gas CO_2 Absorption-Stripping Systems

Hsuan Chang[a]; Chien-Ming Shih[a]
[a] Department of Chemical and Materials Engineering, Tamkang University, Tamsui, Taipei, Taiwan, Republic of China

To cite this Article Chang, Hsuan and Shih, Chien-Ming(2005) 'Simulation and Optimization for Power Plant Flue Gas CO_2 Absorption-Stripping Systems', Separation Science and Technology, 40: 4, 877 — 909
To link to this Article: DOI: 10.1081/SS-200048014
URL: http://dx.doi.org/10.1081/SS-200048014

Separation Science and Technology, 40: 877–909, 2005

ISSN 0149-6395 print/1520-5754 online
DOI: 10.1081/SS-200048014

Simulation and Optimization for Power Plant Flue Gas CO_2 Absorption-Stripping Systems

Hsuan Chang and Chien-Ming Shih
Department of Chemical and Materials Engineering, Tamkang University, Tamsui, Taipei, Taiwan, Republic of China

Abstract: Performance characteristics and design optimization for industrial-scale coal-fired and natural-gas-fired power plant flue gas CO_2 absorption-stripping systems, using MEA (monoethanolamine) and mixed-DGA/MDEA (diglycolamine/methyldiethanolamine) aqueous solutions, are investigated by computer simulation. A rigorous model adopted from the literature, built on RATEFRAC of Aspen Plus, is used to simulate the complex reactive absorption behaviors. Column profiles and mass transfer characteristics as well as the effects of design variables for conventional, conventional with absorber intercooler and split-flow schemes are analyzed. Major design variables for each scheme are identified. Both intercooler and split-flow schemes are beneficial. The split-flow scheme is examined from three aspects for its applicability. Design optimizations by the logical search plan method are performed for both coal-fired and natural-gas-fired CO2 recovery systems using MEA aqueous solution. Compared to practical initial designs, the optimized designs provide cost reductions of 10% and 26% for intercooler and split-flow schemes, respectively.

Keywords: Power plant, carbon dioxide, absorption, stripping, intercooler, split-flow, design optimization, logical search plan, alkanolamine

INTRODUCTION

Control of CO_2 emission from power plants has become an unavoidable issue that requires serious attention due to the Global Warming Problem. According to

Received November 3, 2003, Accepted October 21, 2004.
Address correspondence to Hsuan Chang, Department of Chemical and Materials Engineering, Tamkang University, 151 Ying-Chuan Road, Tamsui, Taipei 25137, Taiwan, Republic of China. E-mail: nhchang@mail.tku.edu.tw

IEA's report (1), compared to other technologies, CO_2 absorption using various amine solutions is most feasible. However, CO_2 recovery system places significant economic impact on the power plant. The increase of electricity cost can be as high as 75% and the plant efficiency can be lowered by 26∼38% (2, 3). At present, there have been only few industrial recovery plants built and operated, the oldest plant at Kerr-McGee Chemical Co. located at Trona, California (4).

Acid gas absorption, in particular for CO_2 and H_2S, using various alkanolamine solutions has been a sophisticated technology in refinery and gas industries (5). There have been in-depth researches in almost all related fundamental aspects, including chemical kinetics, thermodynamic equilibrium as well as mathematical model developments (6–11). Although most of the researches emphasized the absorption process, the theoretical fundamentals are equally well applicable to both absorption and stripping.

The reactive absorption behaviors are highly complex in nature because multiple equilibrium and kinetic reversible chemical reactions are involved in the heat and mass transfers. The model developed by Pacheco and Rochelle (11) is built upon RATEFRAC, the rate-based distillation module of Aspen Plus. User-supplied subroutines for heat and mass transfer coefficients are incorporated into RATEFRAC to account for the chemical reaction effects. This model is highly suitable for simulating the industrial CO_2 recovery system due to the model's rigorous theoretical fundamentals and the flexibility of Aspen Plus to incorporating various process configurations.

Compared to the conventional absorber-stripper scheme, adding an absorber intercooler and using the split-flow arrangement are potential configuration modifications for energy saving (5). Absorber intercooler allows a greater solute build-up in the rich solvent, and thereby reducing the total solvent circulation rate. With split-flow scheme, the amount of circulated absorber liquor that requires more stringent regeneration might be reduced. Thompson and King (12) have investigated the characteristics of absorption-stripping systems that apply absorber intercooling or split-flow designs. The solute to be absorbed is CO_2 or H_2S and the solvent is MEA (monoethanolamine) or DEA (diethanolamine) aqueous solution. They concluded that the optimal location of intercooler is near halfway absorption point at absorber and split-flow can only provide energy savings for absorber-limited systems with constraints on rich solvent loading. Because CO_2 absorption using MEA or DEA is stripper-limited, there is no energy-saving potential for applying split-flow design.

Considering the significant cost impacts on power plant operations, design optimization is crucial for the power plant flue gas CO_2 absorption-stripping systems. Despite the complex chemical absorption/stripping, the literature reported studies on the effects of various design variables used equilibrium models, such as HYSIM and Aspen Plus, which cannot realistically predict the performances of the absorber and the stripper (4, 13). This paper presents the results of performance characterization and design optimization for an industrial-scale power plant flue gas CO_2 absorption-stripping system using the above-mentioned model (11). The feed gas conditions listed in Table 1, illustrated in Desideri and Paolucci (13), for a typical 320 MW coal-fired and natural-gas-fired steam power plant, are used in this study. The solvents investigated are MEA aqueous solution and 50 wt% DGA/MDEA mixed-amine aqueous solution; the former is most commonly used mainly due to its high reactivity and low cost, while the latter gains great attention in recent years due to its high reactivity and low regeneration energy consumption (5). For performance characteristics study, base cases are defined where the absorber and the stripper using Pall ring packings are sized according to common engineering practices. Column profiles, mass transfer characteristics, and design variable sensitivity analysis are studied for conventional, conventional with absorber intercooler, and split-flow schemes. For split-flow scheme, its applicability are examined from three aspects, including feed and design conditions, operation and equilibrium relations, and reboiler duty dependent characteristics. Because too many design variables are involved and the system involves complex mathematical models as well as multiple process units, applying pure mathematical search for the optimization is not feasible. In this study, a systematic search method, the logical search plan method (14) is adopted for the optimization of two potentially advantageous configurations, the conventional with absorber intercooler scheme, and the split-flow with absorber intercooler scheme.

MATHEMATICAL MODEL

The reactive absorption behaviors of the CO_2-alkanolamine-H_2O system are highly complex because of the multiple equilibrium and kinetic reversible reactions. The kinetic reversible reactions involved are:

$$CO_2 + OH^- \overset{k_{OH}}{\longleftrightarrow} HCO_3^- \qquad K_{OH} \tag{1}$$

Table 1. Flue gas conditions

Conditions	Fuel: Coal	Fuel: Natural gas
Feed pressure (bar)	1.0	1.0
Temperature (°C)	66.5	66.5
Flow rate (kmol/hr)	4,330	4,330
Composition (mole fraction)		
CO_2	0.132	0.080
H_2O	0.062	0.062
N_2	0.758	0.810
O_2	0.048	0.048

for primary or secondary alkanolamines:

$$CO_2 + H_2O + R_1R_2NH \overset{k_{2p}}{\longleftrightarrow} R_1R_2NCOO^- + H_3O^+ \qquad K_{2p} \tag{2}$$

for tertiary alkanolamines:

$$CO_2 + H_2O + R_1R_2R_3N \overset{k_{2t}}{\longleftrightarrow} R_1R_2R_3NH^+ + HCO_3^- \qquad K_{2t} \tag{3}$$

The equilibrium reactions involved are:

$$2H_2O \Longleftrightarrow H_3O^+ + OH^- \qquad K_w \tag{4}$$

$$CO_2 + 2H_2O \Longleftrightarrow HCO_3^- + H_3O^+ \qquad K_{CO_2} \tag{5}$$

$$CO_3^{-2} + H_2O \Longleftrightarrow HCO_3^- + OH^- \qquad K_{bic} \tag{6}$$

$$R_1R_2R_3N + H_2O \Longleftrightarrow R_1R_2R_3NH^+ + OH^- \qquad K_{R3N} \tag{7}$$

In this study, the point model as well as the framework for incorporating the model into RATEFRAC both developed by Pacheco and Rochelle (11) are adopted for simulating the packed-tower absorber and stripper. The point model predicts the enhancement factors and actual mass transfer coefficients for each segment of the column, while RATEFRAC is the rate-based distillation module of Aspen Plus that uses the Generalized Maxwell-Stefan approach to multicomponent mass transfer. The point model uses the approximate analytical expression for the enhancement factor, which is derived by DeCoursey (15) for reversible second-order chemical reactions based on the surface renewal theory (16). Detail formulations and experimental verifications for the model, for both absorption and desorption, were reported in Pacheco's dissertation (17).

Pall ring packings are used in both absorption and stripping columns. Physical mass transfer coefficients for liquid and vapor as well as the interfacial area for Pall ring packings are estimated using Bravo and Fair's correlation (18). The heat transfer coefficients for liquid and vapor are estimated by Chilton-Colburn analogy (19). Redlich-Kwong-Soave equation of state (20) and electrolyte-NRTL (21) models are used to represent the thermodynamic equilibriums of vapor and liquid, respectively. The methods and correlations used by Austgen (22) and Pocheco (17) are followed for the estimation of the physical and transport properties for the CO_2-MEA-H_2O and CO_2-DGA-MDEA-H_2O systems.

SYSTEM PERFORMANCE CHARACTERISTICS ANALYSIS

The performance characteristics analysis focuses on coal-fired flue gas condition and uses 20 wt% MEA aqueous solution or 25 wt%/25 wt% DGA/MDEA aqueous solution with lean solvent loadings of 0.15 and 0.1, respectively. The loading represents the molar ratio of total CO_2 related species to total amine related species in the solution. The removal efficiency for CO_2 is set at 90%.

Three different system configurations are examined, including the conventional, conventional with absorber intercooler, and split-flow schemes, as shown in Fig. 1. Heat integration between lean solvent and rich solvent is included considering counter-current heat exchanger with the minimum temperature difference of 5°C. The temperatures of lean solvent entering the absorber and of rich solvent entering the stripper are set at 40°C and 90°C, respectively. The stripper condenser temperature is set at 70°C.

Column simulation results from different segment height settings indicate that column performances do not show distinguishable differences for segment height less than 60 cm, therefore segment height of 50 cm is used throughout this study. Column sizing results for 70% flooding are listed in Table 2.

Conventional Scheme

Basic column profiles for the absorbers are shown in Fig. 2. The bulk of CO_2 gas is absorbed near the top of the absorber (Figs. 2-a, 2-d) and consequently the temperature bulge is located near the top (Figs. 2-b, 2-e) due to the absorption heat effect. However, when the liquid flow rate is increased, the location of the bulge will move downward as discussed in Kohl and Nielsen (5). Due to its lower heat of reaction, the bulge is broader and the vapor and liquid temperatures are lower for the DGA/MDEA solution case as compared to the MEA solution case. As for the mass transfer resistances, resistances from both liquid and vapor phases are significant for the MEA solution case (Fig. 2-c), but the liquid phase resistance is relatively higher. On the other hand, mass transfer resistance from vapor phase is negligible for the DGA/MDEA solution case (Fig. 2-f). The liquid phase, vapor phase, and overall mass transfer resistances are defined as:

$$R_L = \frac{1}{E \cdot k_L^o} \tag{8}$$

$$R_G = \frac{R \cdot T}{k_G \cdot \mathrm{H}} \tag{9}$$

$$R_O = R_L + R_G \tag{10}$$

In Eq. (8), the enhancement factor (E) is defined as the ratio of the actual mass transfer flux, which is enhanced by chemical reaction, to the physical mass transfer flux.

Basic column profiles for the strippers are shown in Fig. 3. Mass transfers of CO_2 are evenly distributed along the entire column, but rates are still higher

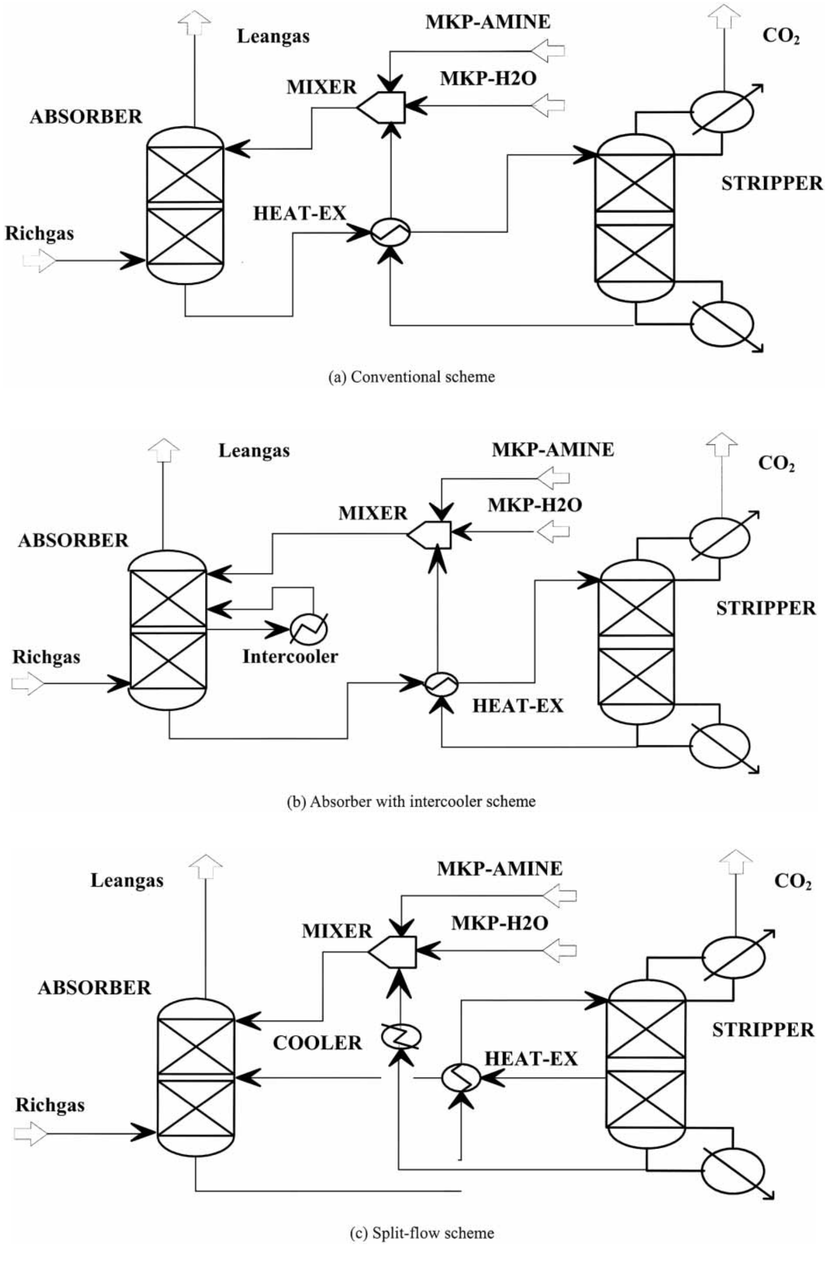

Figure 1. Flow schemes.

Table 2. Design conditions for conventional scheme

	Solution	
Conditions	MEA	DGA/MDEA
Flue gas		
T (°C)	66.50	66.50
P (bar)	1.0	1.0
Flow rate (kmol/hr)	4,330	4,330
y_{CO_2}	0.132	0.132
Lean solvent		
T (°C)	40.01	40.00
P (bar)	1.0	1.0
Flow rate (kg/hr)	6,11,645.45	7,04,627.17
W_{AM} (wt%)	20	25/25
α_{ls}	0.15	0.1
Absorber design		
Total packing height (m)	12	10
Total Segment No.	24	20
Diameter (m)	5.4	5.0
Stripper design		
Total packing height (m)	14	8
Total Segment No.	28	16
Diameter (m)	4.4	4.0
Condenser temperature (°C)	70.00	70.00

near the top section (Figs. 3-a, 3-d). The temperature profiles are monotonously decreasing from bottom to top of the stripper (Figs. 3-b, 3-e). Mass transfer resistances from both liquid and vapor phases are significant for both MEA solution and DGA/MDEA solution cases (Figs. 3-c, 3-f). However, vapor phase contribution is higher for the former while liquid phase contribution is higher for the latter.

Sensitivity analysis is conducted to explore the effects of major system design and operating variables on the stripper reboiler duty and the total operating cost. The total operating cost includes (1) utility costs from condenser, reboiler, trim cooler, trim heater, and feed gas compression, and (2) amine costs due to losses from exit gases from both columns. Pumping costs are neglected. The unit prices of utilities and amines are listed in Table 3. The equipment cost is not considered because it is the operating cost that places significant impact on the electricity generation cost.

Because the utility cost of reboiler dominates the total operating cost, the effect characteristics are similar as shown in Fig. 4. The variables with most significant impacts are lean solvent loading, feed gas CO_2 mole fraction, absorber pressure, and stripper pressure. Lowering lean solvent

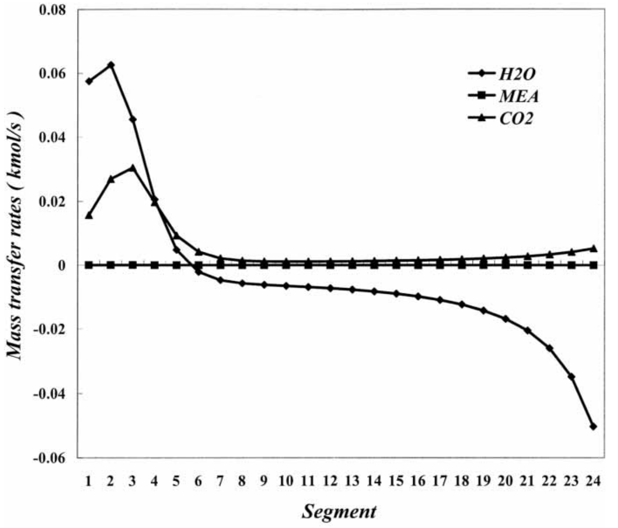

(a) Mass transfer rate profiles (20 wt% MEA)

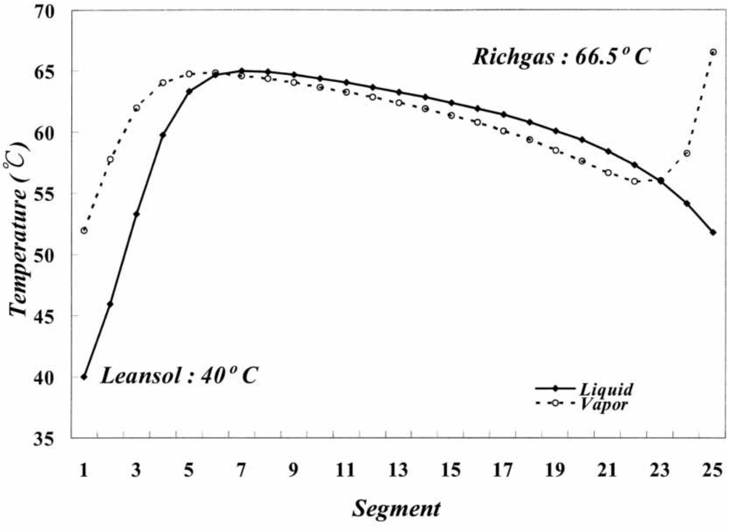

(b) Temperature profiles (20wt% MEA)

Figure 2. Absorber column internal profiles—conventional scheme.

(*continued*)

loading has the greatest effect, but the effect of raising loading is much less. Feed gas CO_2 mole fraction shows linear impact. Raising absorber pressure provides no advantages due to high compression costs. For DGA/MDEA solution system, lowering stripper pressure is favorable. However, for the

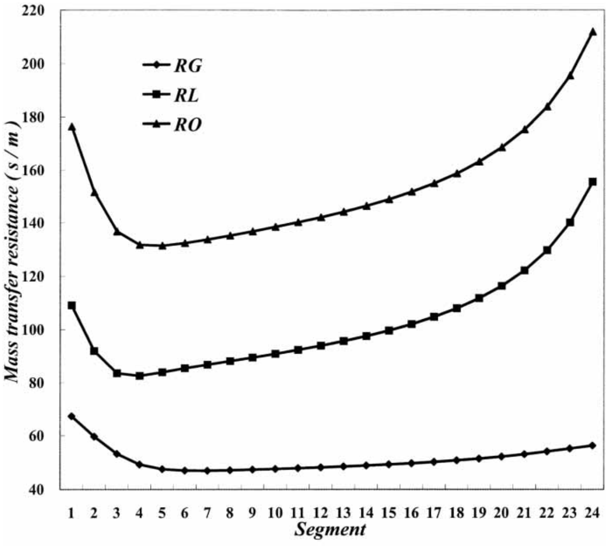

(c) Mass transfer resistance profiles (20wt%MEA)

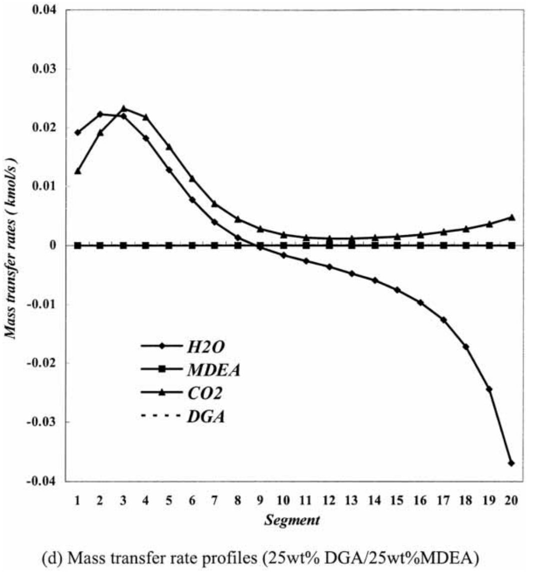

(d) Mass transfer rate profiles (25wt% DGA/25wt%MDEA)

Figure 2. Continued.

20 wt% MEA solution system, an optimal stripper pressure can be found. Further analysis indicates that for the 30 wt% MEA solution system, the effect of stripper pressure is similar to that of DGA/MDEA solution system. Raising operation pressure should result in the relief of pinch

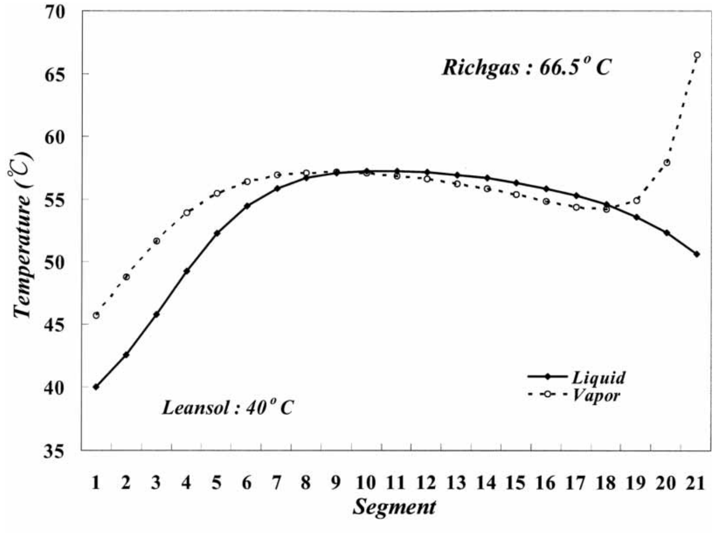

(e) Temperature profiles (25wt% DGA/25wt%MDEA)

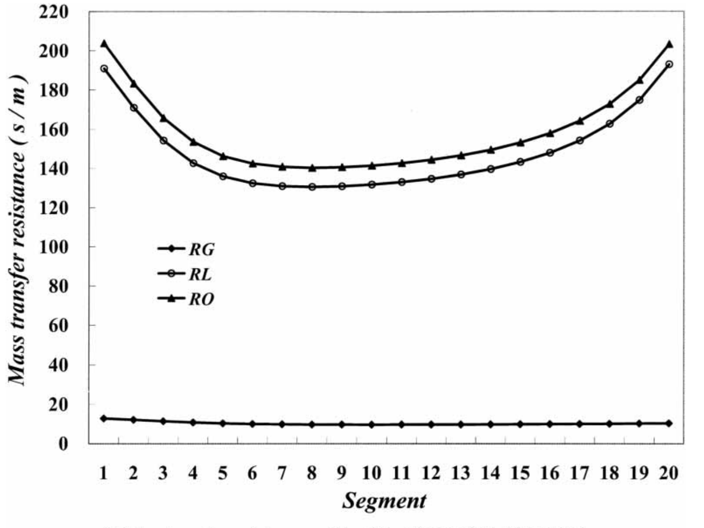

(f) Mass transfer resistance profiles (25wt% DGA/25wt%MDEA)

Figure 2. Continued.

phenomena at the bottom of stripper and consequently reduction of reboiler duty. The existence of an optimal stripper pressure is resulted from the solvent loading constraints, which limits the reduction of the vapor-liquid flow ratio.

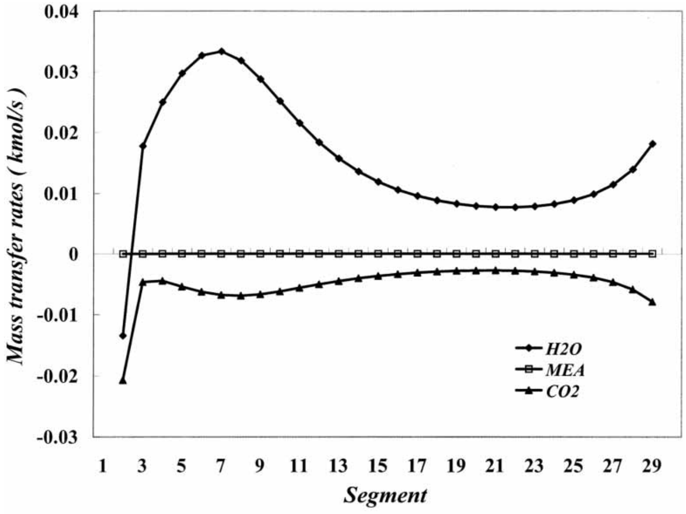

(a) Mass transfer rate profiles (20wt% MEA)

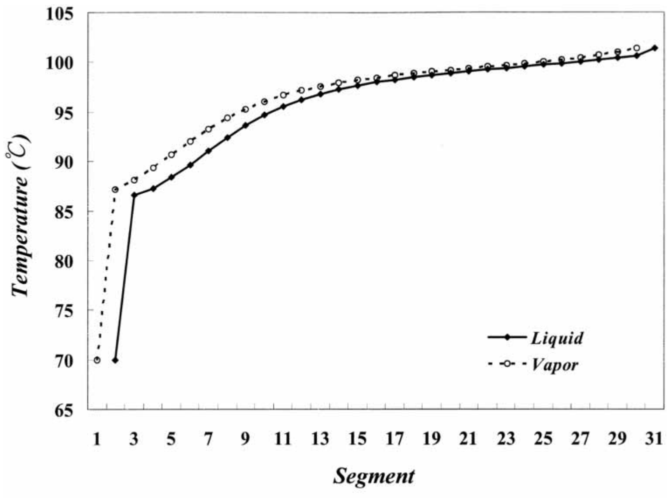

(b) Temperature profiles (20wt% MEA)

Figure 3. Stripper column internal profiles—conventional scheme.

(*continued*)

Conventional with Absorber Intercooler Scheme

Considering addition of a cooler at an appropriate location for the absorber, the intercooler location is parameterized by F_I, which is defined as the

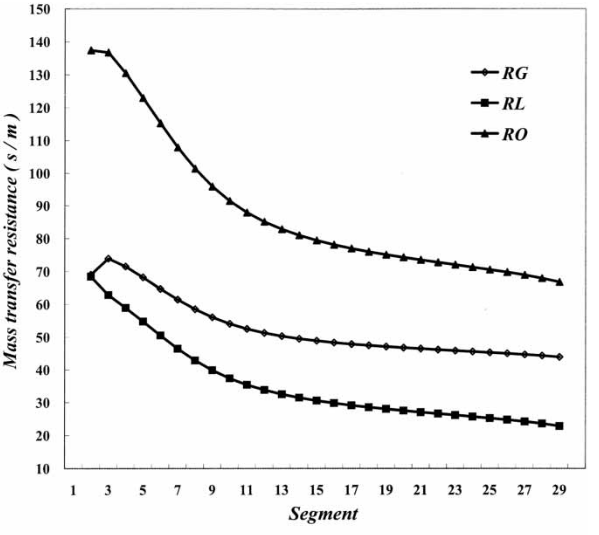

(c) Mass transfer resistance profiles (20wt%MEA)

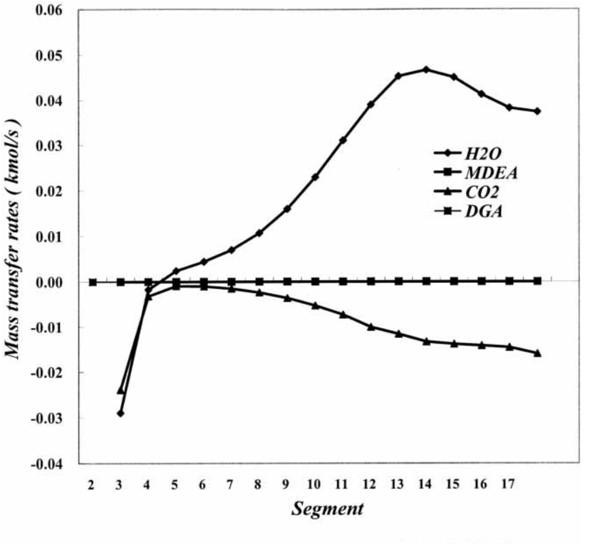

(d) Mass transfer rate profiles (25wt% DGA/25wt%MDEA)

Figure 3. Continued.

degree of lean solvent enrichment up to the intercooler location relative to the entire column enrichment (12).

$$F_I = \frac{\alpha_{ic} - \alpha_{ls}}{\alpha_{rs} - \alpha_{ls}} \tag{11}$$

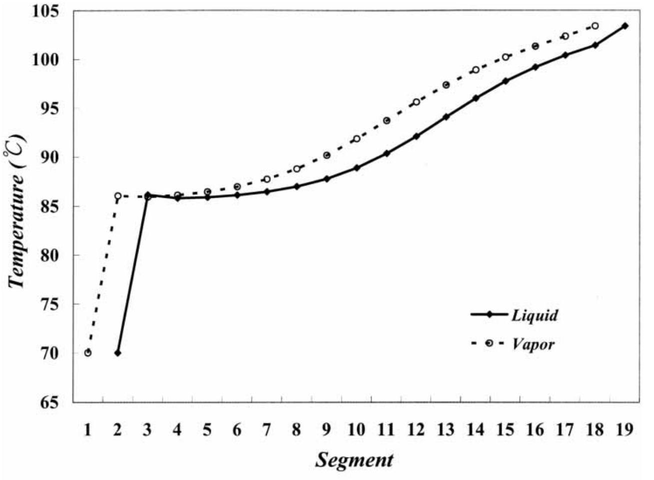

(e) Temperature profiles (25wt% DGA/25wt%MDEA)

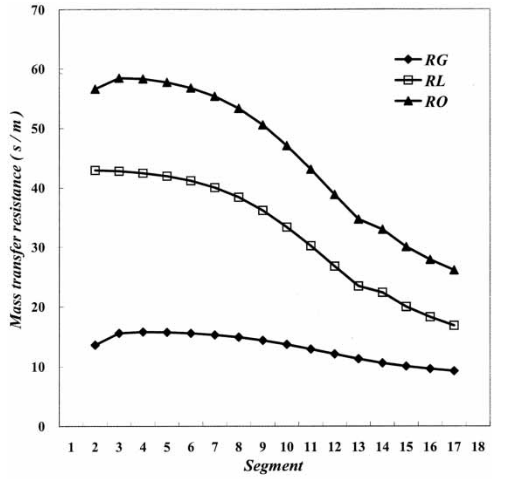

(f) Mass transfer resistance profiles (25wt% DGA/25wt%MDEA)

Figure 3. Continued.

Table 3. Unit prices of utilities and alkanoamines (5)

Utility/amine	Unit cost
Cooling Water[a] (US$/GJ)	0.16
Steam[a] (US$/GJ)	3.17
MEA (US$/kg)	1.3
DGA (US$/kg)	2.0
MDEA (US$/kg)	3.1

[a]cost per unit amount of heat exchange.

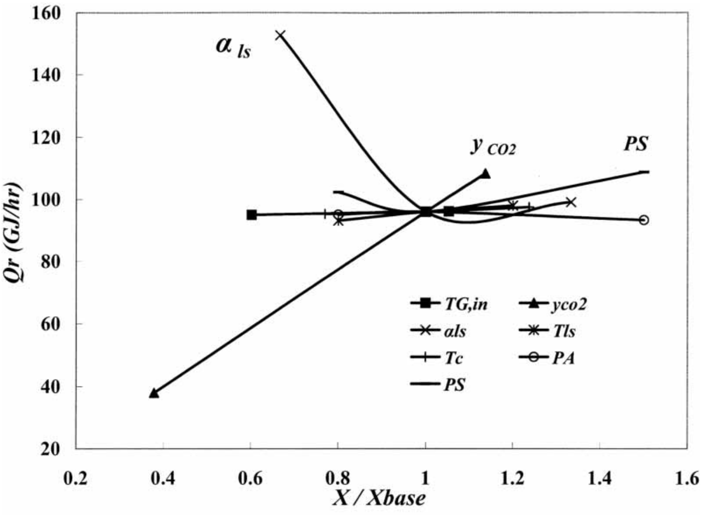

(a) Effects on reboiler duty (20wt% MEA)

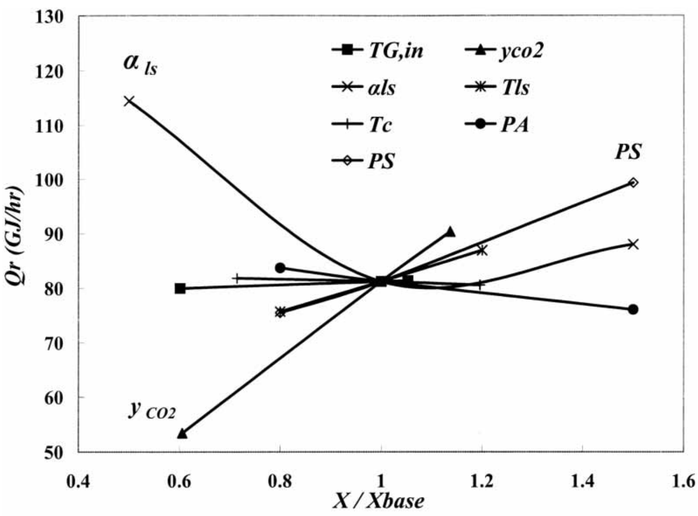

(b) Effects on reboiler duty (25wt% DGA/25wt%MDEA)

Figure 4. Effects on reboiler duty and total cost—conventional scheme. (*continued*)

For the above-mentioned base case at F_I value of 0.5 and the liquid withdrawn is cooled to 40°C before returning to the absorber, mass transfer rate and temperature profiles of absorber are shown in Fig. 5. Compared to the conventional design, major absorption still occurs at upper sections and

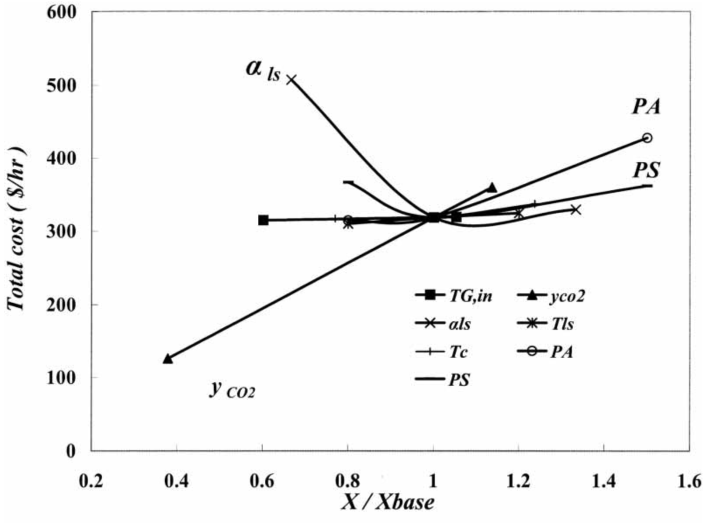

(c) Effects on total cost (20wt% MEA)

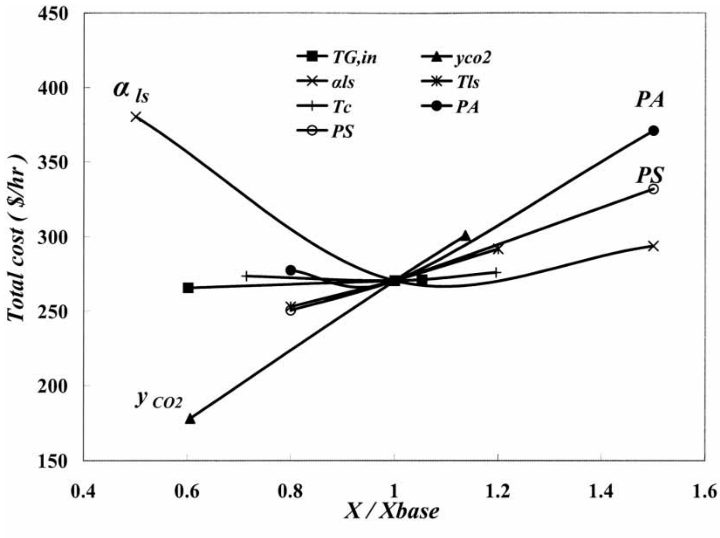

(d) Effects on total cost (25wt% DGA/25wt%MDEA)

Figure 4. Continued.

mass transfer rates near intercooler are significantly increased for MEA system. Average temperature reduction is about 10∼15°C for the column, and temperature bulge does not exist anymore. Due to the reduction in required solvent circulation rate, the stripper reboiler duty is reduced and so

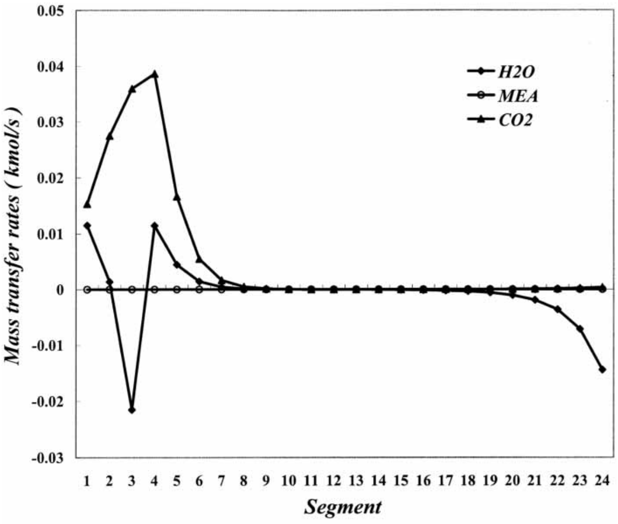

(a) Mass transfer rate profiles ($F_I = 0.55$, 20wt% MEA)

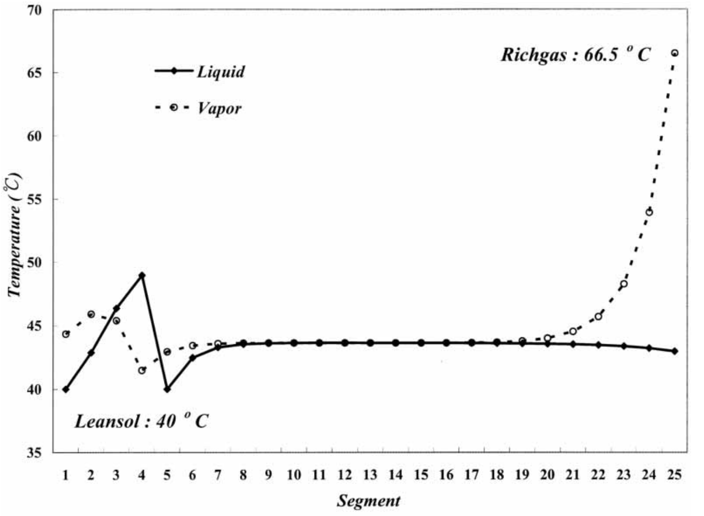

(b) Temperature profiles ($F_I = 0.55$, 20wt% MEA)

Figure 5. Absorber column internal profiles—intercooler scheme. (*continued*)

is the total operating cost. The effects of intercooler location, expressed by F_I, are shown in Fig. 6. Intercooler located near the bottom provides the highest benefits because the pinch near the bottom, implied from Fig. 5a and Fig. 5c, can be relaxed.

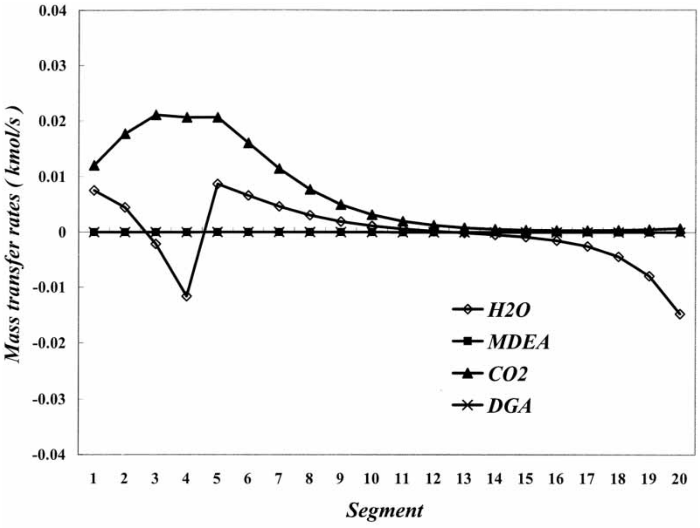

(c) Mass transfer rate profiles (F_I = 0.5, 25wt% DGA/25wt%MDEA)

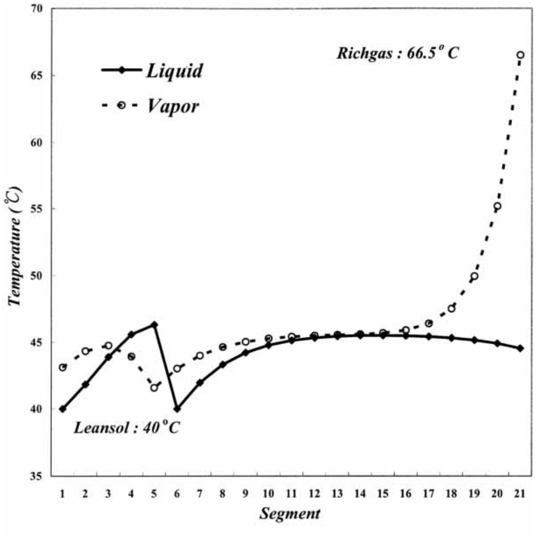

(d) Temperature profiles (F_I = 0.5, 25wt% DGA/25wt%MDEA)

Figure 5. Continued.

Split-Flow Scheme

In split-flow scheme, a portion of internal liquid is withdrawn from an intermediate location of stripper and added into an intermediate location of

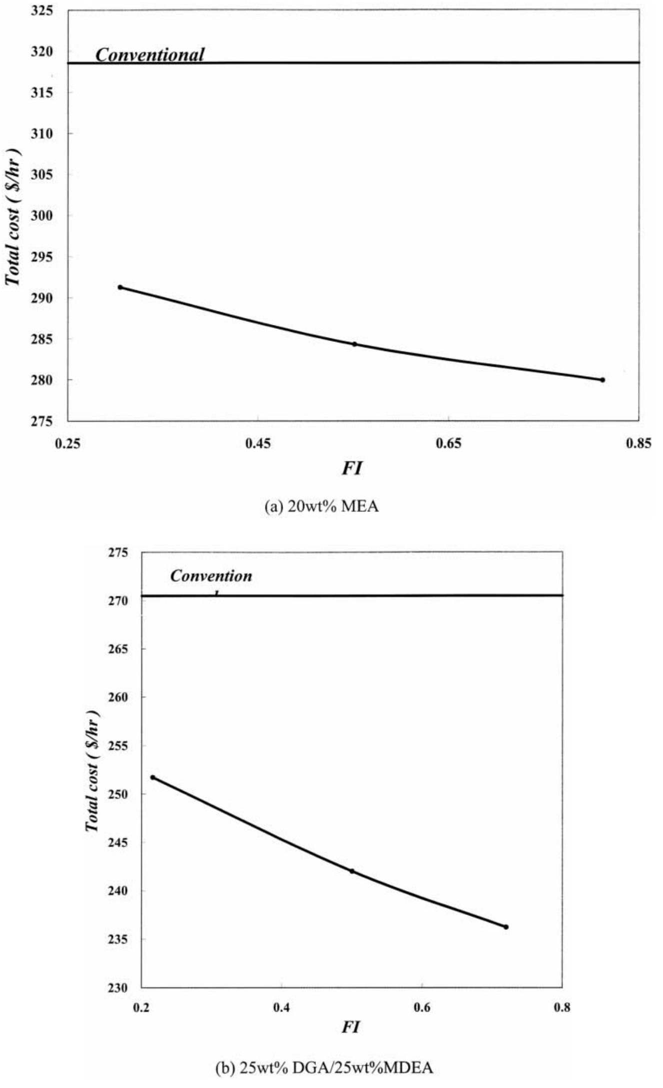

(a) 20wt% MEA

(b) 25wt% DGA/25wt%MDEA

Figure 6. Effects on intercooler location.

absorber. Parameters Fc_A and Fc_S, defined similarly to F_I, are used to express the split stream adding and drawing locations in the absorber and stripper (12).

$$Fc_A = \frac{\alpha_a - \alpha_{ls}}{\alpha_{rs} - \alpha_{ls}} \tag{12}$$

$$Fc_S = \frac{\alpha_s - \alpha_{ls}}{\alpha_{rs} - \alpha_{ls}} \tag{13}$$

In this study, it is set that Fc_A is equal to Fc_S and Fc is used to denote the side-draw location.

Split-flow scheme allows portion of absorption liquid to be regenerated less stringently; however, the required total circulation liquid rate must be increased. Therefore, the overall impact on stripper reboiler duty, which dominates the total operating cost, is not always beneficial. The applicability of split-flow scheme is examined from three aspects in this study, including feed and design conditions, operation and equilibrium relations, and reboiler-duty dependent characteristics. The effects of parameters pertaining to the split-flow on total costs are provided.

Feed and Design Conditions

Feed gas CO_2 mole fractions of 0.132 and 0.08, corresponding to coal-fired and natural-gas-fired flue gases, with removal efficiencies of 90% and 95% are analyzed. The effects of lean solvent loading on stripper reboiler duty and total cost are shown in Fig. 7. Split-flow scheme provides greater benefit when lean solvent loading is set at a more stringent level. Compared to the conventional scheme, up to about 20% reduction in stripper reboiler duty and total cost can be obtained for the analyzed cases.

Operation and Equilibrium Relations

Following Thompson and King (12), the characteristics of conventional and split-flow schemes can be compared via operating diagrams, which include equilibrium curve, operating curve, and efficiency curve. The equilibrium curve is determined by the liquid phase composition and its corresponding temperature at each point of the column. The operating curve represents the actual compositions of the contacting vapor and liquid streams at each point of the column. The efficiency curve relates the actual compositions of the two streams leaving a given point of the column. The distance between operating and equilibrium curves represents the driving force for mass transfer, while the distance between efficiency curve and equilibrium curve reflects the efficiency of vapor-liquid mass transfer. Besides, the slope of operating curve represents the ratio of vapor and liquid flow rates.

The operating diagrams for both conventional and split-flow schemes are given in Fig. 8 and Fig. 9. Comparing these two sets of figures, one can find out that: (1) severe pinch characteristics occur at the bottom sections of both absorber and stripper, particularly for the stripper; and (2) split-flow scheme allows different slopes of the operating curve for the top and bottom sections of the column, which corresponds to the vapor-liquid flow ratios. In split-flow scheme, the stripper reboiler duty can be reduced due to both the change of operating curve slope at the top section of the stripper and the reduction of liquid flow at the bottom section of the stripper from splitting of liquid flow.

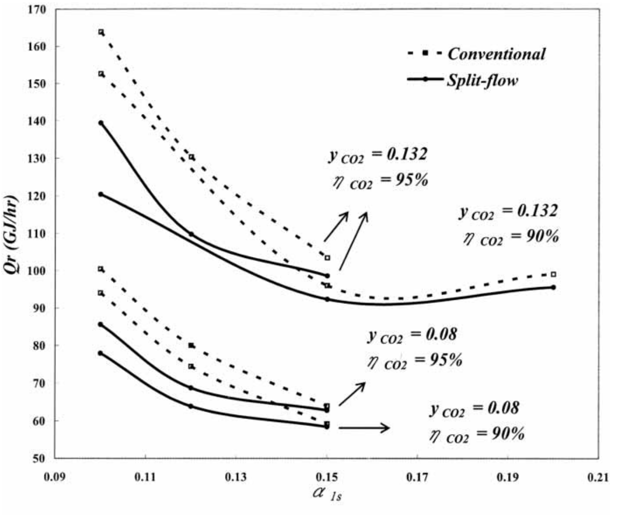

(a) Effects on reboiler duty (20wt%MEA)

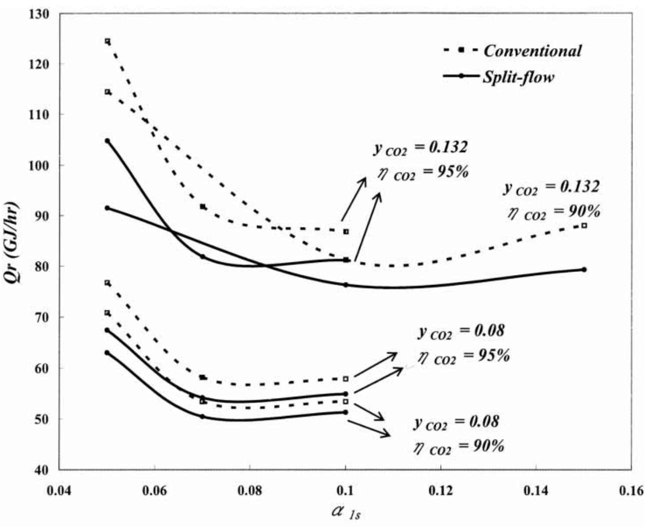

(b) Effects on reboiler duty (25wt% DGA/25wt%MDEA)

Figure 7. Effects of feed and design conditions—split-flow scheme.

(*continued*)

Reboiler Duty Dependent Characteristics

According to the nature of stripper reboiler duty dependent characteristics, Thompson and King (12) distinguished the absorber-stripper systems into

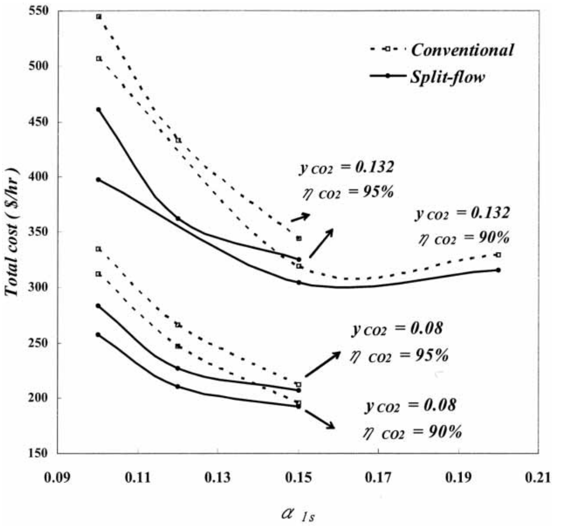

(c) Effects on total cost (20wt%MEA)

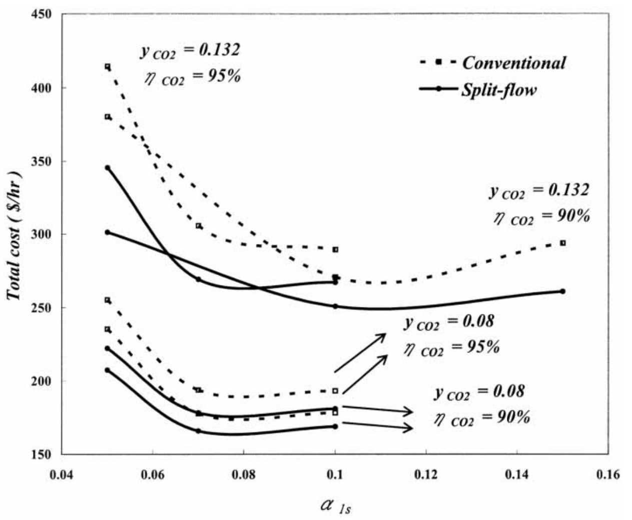

(d) Effects on total cost (25wt% DGA/25wt%MDEA)

Figure 7. Continued.

absorber-limited and stripper-limited. Absorber-limited systems have strippers that exhibit a minimum steam consumption for the lowest total solvent flow rate, while stripper-limited systems exhibit an internal-minimum steam consumption with respect to the total solvent flow rate and

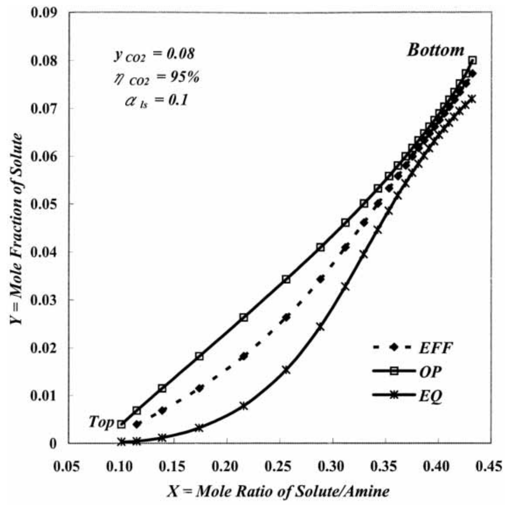

(a) Absorber operating diagram (20wt%MEA)

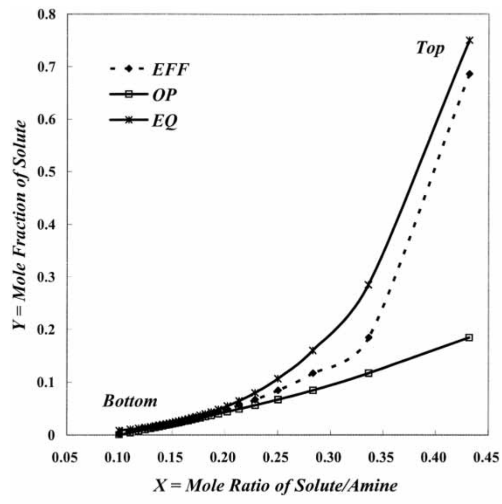

(b) Stripper operating diagram (20wt%MEA)

Figure 8. Operating diagrams—conventional scheme.

(*continued*)

the lean solvent loading. They concluded that split-flow schemes provide energy savings only for absorber-limited systems with maximum solvent loading constraints, and all CO_2 systems are stripper-limited.

For the base cases analyzed in this study, CO_2/MEA and CO_2/DGA/MDEA systems are stripper-limited, as shown in Fig. 10. However, it is

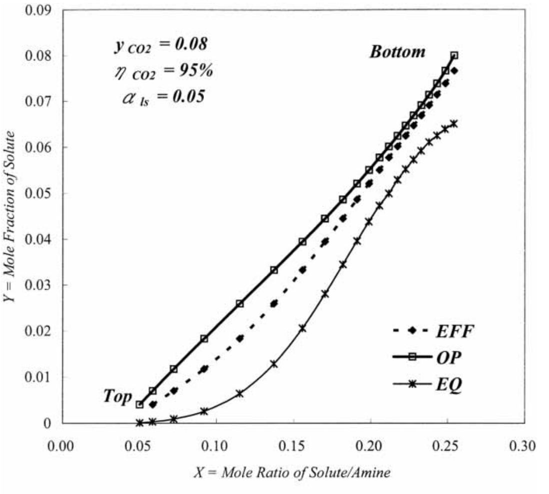

(c) Absorber operating diagram (25wt% DGA/25wt%MDEA)

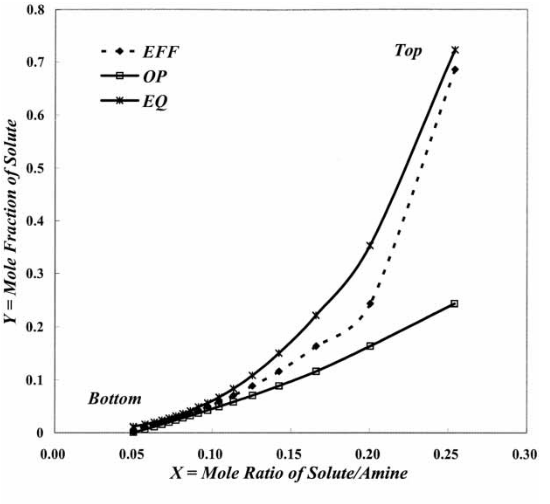

(d) Stripper operating diagram (25wt% DGA/25wt%MDEA)

Figure 8. Continued.

indicated in Fig. 7 that split-flow schemes are still capable of providing benefits, in particular for the DGA/MDEA system.

Parameter Studies

The parameters investigated are lean solvent loading, split flow rate, and location (*Fc*). The effects on total costs are shown in Fig. 11. Lean solvent

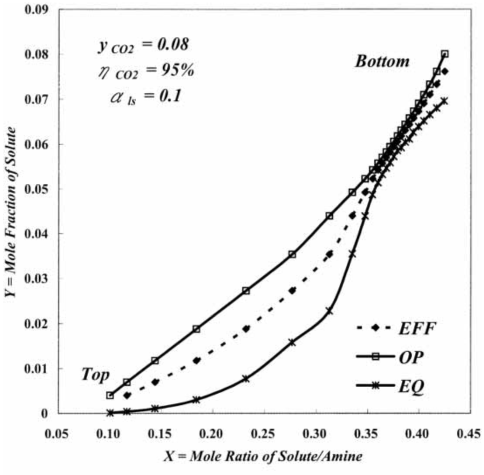

(a) Absorber operating diagram

(20wt%MEA, Fc_A =0.543, Fc_S =0.534, L_{Side} =130000kg/hr)

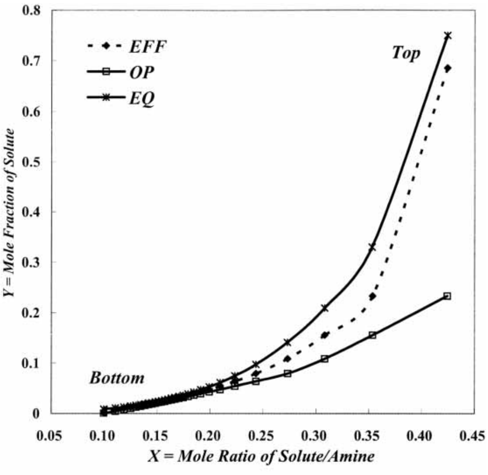

(b) Stripper operating diagram

(20wt%MEA, Fc_A =0.543, Fc_S =0.534, L_{Side} =130000kg/hr)

Figure 9. Operating diagrams—split-flow scheme.

(*continued*)

loading shows greatest impact and reducing *Fc*, i.e., split stream is at a lower location in the stripper and can result in lower cost. The impact of split flow rate is less significant than the other two parameters. Comparing base cases only, the split-flow schemes provide cost reductions of 15% and 12.6% for MEA and DGA/MDEA systems, respectively.

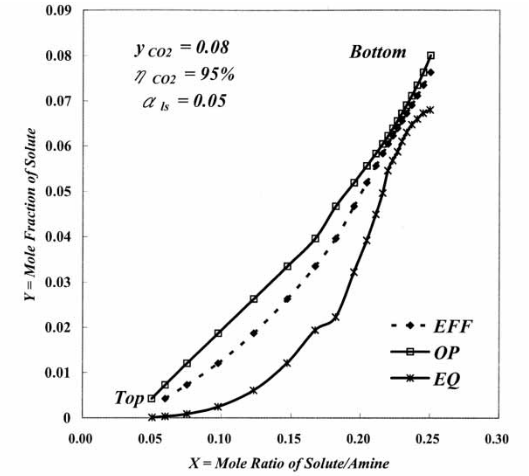

(c) Absorber operating diagram

(25wt% DGA/25wt%MDEA, Fc_A =0.586, Fc_S =0.536, L_{Side} =146800kg/hr)

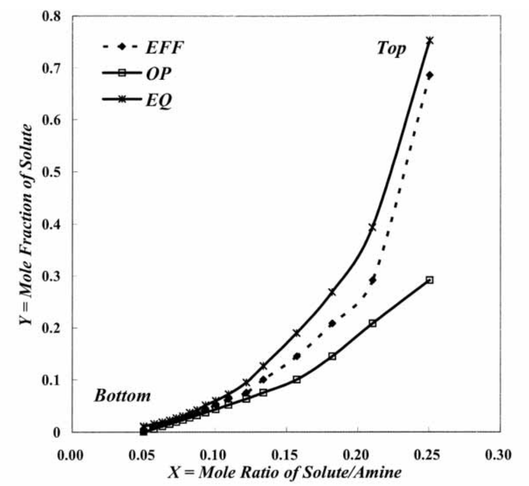

(d) Stripper operating diagram

(25wt% DGA/25wt%MDEA, Fc_A =0.586, Fc_S =0.536, L_{Side} =146800kg/hr)

Figure 9. Continued.

DESIGN OPTIMIZATION

Since schemes with intercooling and split-flow are both beneficial from the above studies, design optimizations for these two schemes are performed to find out the design conditions with lowest total cost.

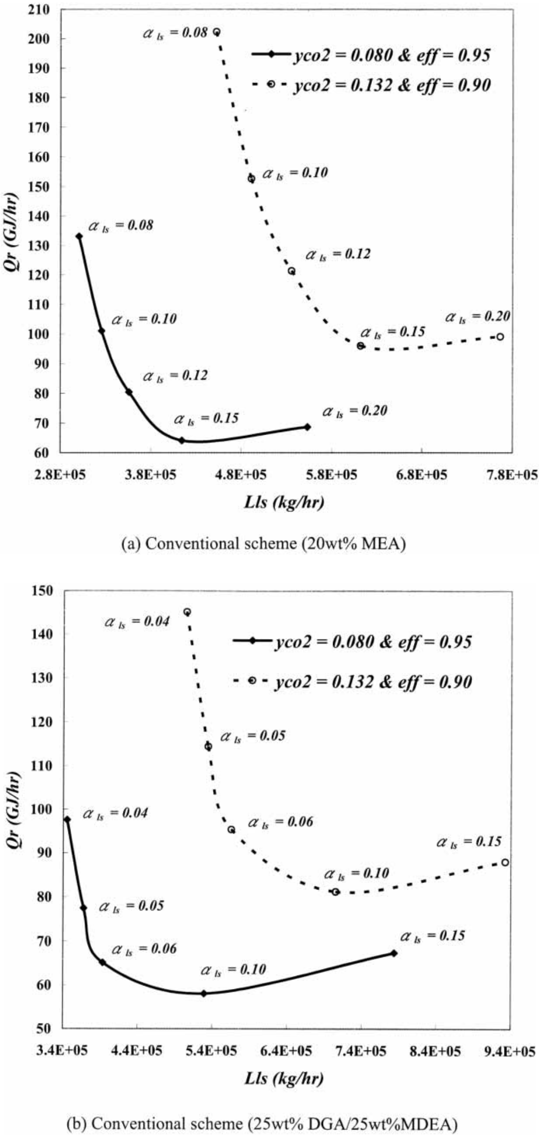

Figure 10. Reboiler duty characteristics.

Logical Search Plan Method

The system to be optimized involves many variables and the prediction of system performance relies on complex modular mathematical model, so a pure mathematical search approach is not appropriate. In this study, a

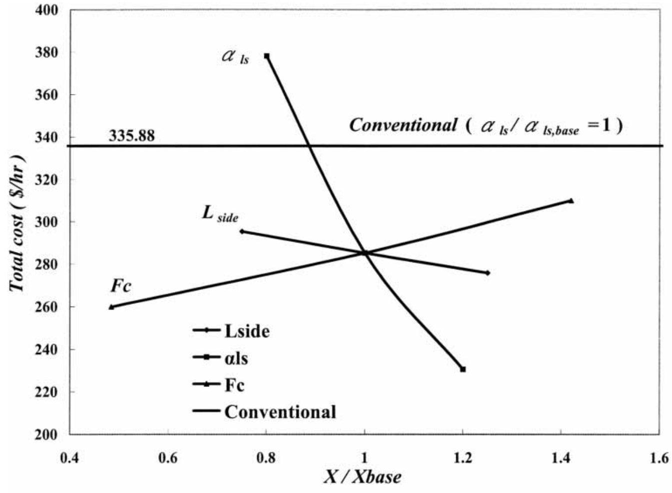

(a) 20wt% MEA

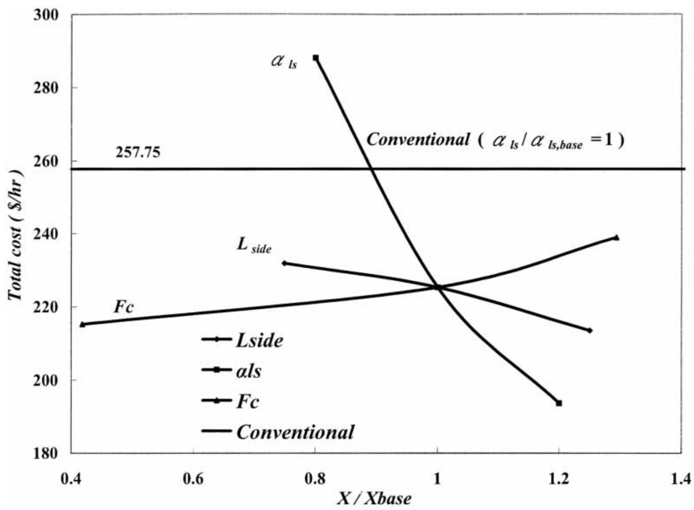

(b) 25wt% DGA/25wt%MDEA

Figure 11. Effects of design variables—split-flow scheme.

logical search plan method (14) is used. Starting with an initial design and defined search increment, an exploratory design search is conducted by changing each design variable in turn to find out improved design. Pattern design search is then conducted by changing the design variables in the conjecture directions based on the exploratory design search. The search flow diagram is depicted in Fig. 12.

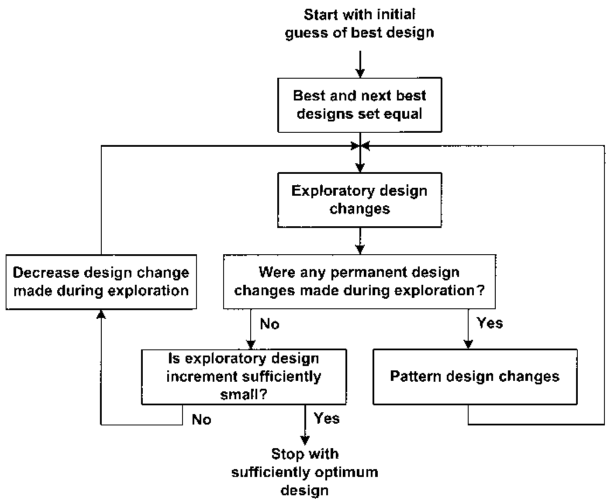

(a) Logical search plan

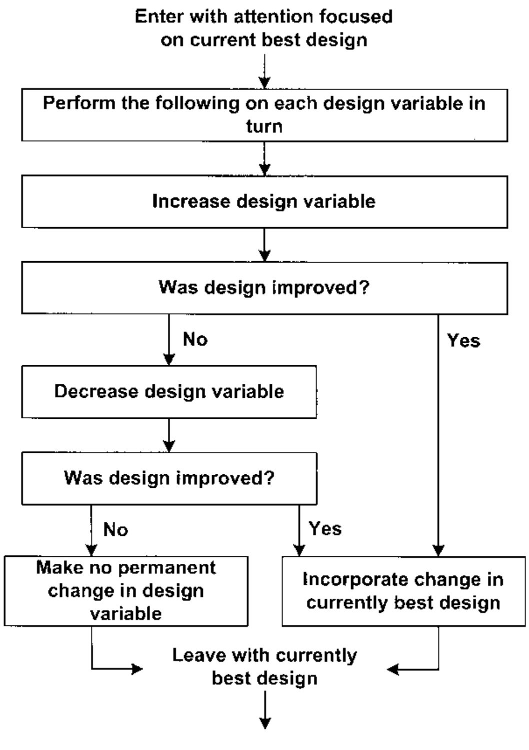

(b) Exploratory design changes

Figure 12. Logical search plan method flow diagrams.

(*continued*)

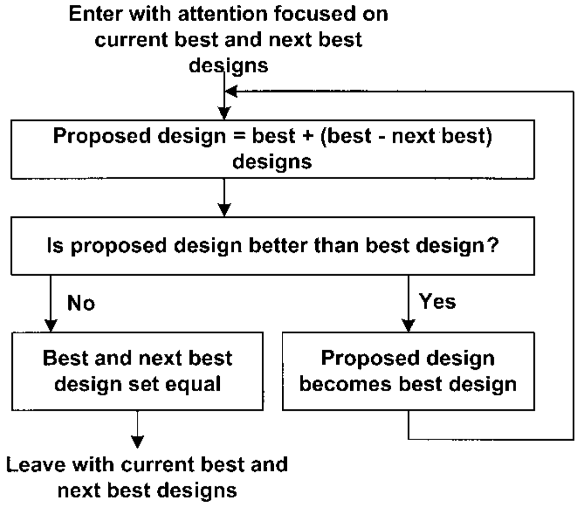

(c) Pattern design changes

Figure 12. Continued.

Conventional with Absorber Intercooler Scheme

The absorption-stripping system of conventional with absorber intercooler scheme for treating coal-fired flue gas with CO_2 composition of 13.2% using MEA aqueous solvent is optimized. The CO_2 recovery requirement is set at 90%. Only major design variables, according to the previous studies, are considered in the optimization. These variables are stripper pressure (*PS*), amine concentration (W_{AM}), lean solvent loading (α_{ls}), intercooler location (F_I), and condenser temperature (T_C). The optimization results are summarized in Table 4. The optimized design uses higher amine concentration, higher lean solvent loading, and the location of intercooler is located near the bottom of the absorber. The cost reduction is 10% compared to the initial design.

Split-Flow with Absorber Intercooler Scheme

For the split-flow with absorber intercooler scheme, the absorption-stripping system for treating natural-gas-fired flue gas with CO_2 composition of 8% using MEA aqueous solvent is optimized. The CO_2 recovery is set at 95%. The major design variables are stripper pressure (*PS*), amine concentration (W_{AM}), lean solvent loading (α_{ls}), intercooler location (F_I), split stream location (*Fc*), split flow rate (L_{side}), and condenser temperature (T_C). The

Table 4. Optimized design for conventional with intercooler scheme

Parameters	Design case: Initial design	Optimized design
PS (bar)	1.0	1.0
W_{AM} (wt%)	20	30
α_{ls}	0.15	0.18
F_I	0.551	0.860
T_C (°C)	70.0	77.5
Total cost (US$/hr)	284.3	254.55

optimized design is shown in Table 5. The optimized design uses higher stripper pressure, higher amine concentration, higher condenser temperature (due to higher stripper pressure), and the locations of both intercooler and split flow are near the bottom of the absorber and the stripper. The cost reduction is 26% compared to the initial design.

CONCLUSIONS

Typical industrial-scale coal-fired and natural-gas-fired power plant CO_2 absorption-stripping systems have been conveniently simulated via a rigorous model built on RATEFRAC of Aspen Plus. The model which allows the complex reactive absorption/stripping behavior of the CO_2-Alkanoamine-H_2O system has been accounted for.

The performance characteristics analysis has been conducted for three schemes, including conventional, conventional with absorber intercooler,

Table 5. Optimized design for split-flow with intercooler scheme

Parameters	Design case: Initial design	Optimized design
PS (bar)	1.0	1.5
W_{AM} (wt%)	20	30
α_{ls}	0.10	0.12
F_I	0.66	0.918
$F_{C,A}/F_{C,S}$	0.481/518	0.141/0.136
L_{side}	1,30,000	1,30,000
T_C (°C)	70.0	82.5
Total cost (US$/hr)	260.5	191.94

and split-flow. The analysis reveals the column internal profiles of temperature and compositions as well as the relative significance of vapor and liquid phase mass transfer resistances. For both absorber and stripper of the MEA system as well as the stripper of DGA/MDEA system, mass transfer resistances from both vapor and liquid phases are equally important. For the absorber of DGA/MDEA system, mass transfer resistance from vapor phase is negligible. The most significant design and operating variables, identified via sensitivity studies, are lean solvent loading, feed gas CO_2 mole fraction, absorber pressure, and stripper pressure. Intercooler scheme is beneficial and its appropriate location is near the bottom of the absorber. Analyses from three aspects indicate that split-flow is beneficial, and when the lean solvent loading is more stringent, greater cost reduction can be obtained.

Logical search plan method has allowed the complex system to be optimized. The optimized designs of intercooler scheme and split-flow with intercooler scheme provide cost reductions of 10% and 26% compared to the initial practical designs.

NOMENCLATURES

E	Enhancement factor
EFF	Efficiency curve
EQ	Equilibrium curve
F_I	Intercooler location parameter
Fc_A	Split-flow location parameter for absorber
Fc_S	Split-flow location parameter for stripper
H	Henry's constant
K	Equilibrium constant
k_G	Gas phase mass transfer coefficient
k_L°	Liquid phase physical mass transfer coefficient
L_{side}	Flow rate of split-flow stream
OP	Operating curve
PA	Absorber pressure
PS	Stripper pressure
R	Gas constant
R_G	Gas phase mass transfer resistance
R_L	Liquid phase mass transfer resistance
R_O	Overall liquid phase mass transfer resistance
T	Temperature
T_C	Condenser temperature
$T_{G,in}$	Inlet gas temperature
T_{ls}	Lean stream temperature
W_{AM}	Amine concentration
y_{CO_2}	Mole fraction of CO_2 in inlet gas

α_A	Split-flow stream solvent loading for absorber
α_S	Split-flow stream solvent loading for stripper
α_{ls}	Lean solvent loading
α_{rs}	Rich solvent loading
η_{CO_2}	Absorption efficiency of CO_2

REFERENCES

1. IEA/OECD. *Carbon Dioxide Capture and Storage*; 2000.
2. Steinberg, M., Cheng, H.C., and Horne, F.. *A Systems Study of the Removal Recovery and Disposal of Carbon Dioxide from Fossil Fuel Power Plants in the U.S.*; U.S. DOE:1984; DOE/CH00016-2.
3. Hendriks, C., Blok, K., and Turkenburg, W. (1990) *Climate and Energy*; Kluwer Academic Press: Netherlands.
4. Chakma, A., Mehrotra, A.K., and Nielsen, B. (1995) Comparison of chemical solvents for mitigating CO_2 emissions from coal-fired power plants. *Heat Recovery Systems & CHP*, 15 (2): 231–240.
5. Kohl, A. and Nielsen, R. (1997) *Gas Purification*; Gulf publishing Company: Houston.
6. Versteeg, G.F. and Swaaij, W.P.M.V. (1988a) On the kinetics between CO_2 and alkanolamines both in aqueous and non-aqueous solutions—I. Primary and secondary amines. *Chem. Eng. Sci.*, 43 (3): 573–585.
7. Versteeg, G.F. and Swaaij, W.P.M.V. (1988b) On the kinetics between CO_2 and alkanolamines both in aqueous and non-aqueous solutions—II. Tertiary amines. *Chem. Eng. Sci.*, 43 (3): 587–591.
8. Austgen, D.M. (1989) *A Model of Vapor–Liquid Equilibria for Acid Gas–Alkanolamine–Water System*; Ph. D. Dissertation: The University of Texas at Austin.
9. Versteeg, G.F., Kuipers, J.A.M., Beckum, F.P.H.V., and Swaaij, W.P.M.V. (1989) Mass transfer with complex reversible chemical reactions—I. Single reversible chemical reaction. *Chem. Eng. Sci.*, 44 (10): 2295–2310.
10. Versteeg, G.F., Kuipers, J.A.M., Beckum, F.P.H.V., and Swaaij, W.P.M.V. (1990) Mass transfer with complex reversible chemical reactions—II. Parallel reversible chemical reaction. *Chem. Eng. Sci.*, 45 (1): 183–197.
11. Pacheco, M.A. and Rochelle, G.T. (1998) Rate-based modeling of reactive absorption of CO_2 and H_2S into aqueous methyldiethanolamine. *Ind. Eng. Chem. Res.*, 37: 4107–4117.
12. Thompson, R.E. and King, C.J. (1987) Energy conservation in regenerated chemical absorption processes. *Chemical Engineering and Processing*, 21: 115–129.
13. Desideri, U. and Paolucci, A. (1999) Performance modelling of a carbon dioxide removal system for power plants. *Energy Conversion & Management*, 40: 1899–1915.
14. Hooke, R. and Jeeves, T.A. (1961) Direct search solution of numerical and statistical problems. *J. Assoc. Comp.*, Mach., **2**: 8.
15. DeCoursey, W.J. (1992) A simpler approximate for enhancement of mass transfer by second-order reversible reaction. In *IChemE. Symp. Ser.*; 128B269–B276.
16. Danckwerts, P.V. (1970) *Gas–Liquid Reactions*; McGraw Hill: New York.

17. Pacheco, M.A. (1998) *Mass Transfer, Kinetics and Rate-Based Modeling of Reactive Absorption*; Ph. D. Dissertation: The University of Texas at Austin.
18. Bravo, J.L. and Fair, J.R. (1982) Generalized correlation for mass transfer in packed distillation columns. *Ind. Eng. Chem. Proc. Des. Dev.*, 21: 162–170.
19. Bird, R.B., Stewart, W.E., and Lightfoot, E.N. (1960) *Transport Phenomena*; John Wiley & Sons, Inc.: New York.
20. Soave, G. (1972) Equilibrium constants from a modified Redlich-Kwong equation of State. *Chem. Eng. Sci.*, 27: 1197.
21. Chen, C.C. and Evans, L.B. (1986) A Local composition model for the excess Gibbs energy of aqueous electrolyte systems. *AIChE Journal*, 32 (3): 444–454.
22. Austgen, D.M. (1989) *A Model of Vapor–Liquid Equilibria for Acid Gas–Alkanolamine–Water System*; Ph. D. Dissertation: The University of Texas at Austin.